tion of alcohol at low conversions. Of course, at equilibrium, the principle of microscopic reversibility requires that both mechanisms contribute equally to the forward and reverse reactions.

Acknowledgment. This work was supported by the Petroleum Research Fund, administered by the American Chemical Society, and by the Army Office of Research (Durham).

Conformational Effects of Sulfur, Silicon, Germanium, and Tin on Alkyl Radicals. An Electron Spin Resonance Study of the Barriers to Internal Rotation

Paul J. Krusic* and Jay K. Kochi*

Contribution No. 1671 from the Central Research Department, E. I. du Pont de Nemours and Company, Wilmington, Delaware 19898, and the Department of Chemistry, Indiana University, Bloomington, Indiana 47401.
Received February 25, 1970

Abstract: The electron spin resonance spectra of a series of alkyl radicals substituted in the β position with sulfur, silicon, germanium, and tin groups are reported. The hyperfine isotropic coupling constants for the β protons are unusually small and show a marked temperature dependence. These results are interpreted in terms of hindered internal rotation about the C_α–C_β bond and a preferred conformational orientation in these radicals in which the sulfur, silicon, germanium, and tin atoms are eclipsed with the p orbital at the trigonal center. These conformational effects are attributed to incipient 1,3 bonding between the unfilled 3d orbitals of the heteroatom and the p orbital of the carbon radical center. A structure involving symmetrically bridged radicals is ruled out. A classical anisotropic averaging of the β hyperfine splitting is discussed and used to determine the heights of the potential barriers hindering rotation in these radicals. The classical treatment of hindered rotation is also applied to simple alkyl radicals. The barrier heights determined by this approach agree with those previously determined by a quantum mechanical treatment. The β hyperfine splittings in the mercaptoalkyl radicals are anomalously small and cannot be accounted for by the unmodified theory. A distorted structure for these radicals is considered in which the β hydrogens are displaced away from their tetrahedral positions. Concomitant with this distortion the sulfur atom is placed closer to the p orbital This model easily explains the anomalously low β-proton splittings. Similar distortions are suggested for simple alkyl radicals. Line-broadening effects in several alkyl and β-substituted alkyl radicals are reported and discussed in terms of the dynamic equilibrium conformations of the radical structures.

Stabilization of alkyl radicals and stereoselectivity in homolytic reactions is a subject which has been considered at length. The effects of a variety of substituents on the steric course of free-radical reactions occupies a prominent position in these investigations. Substituents located in the β position generally exert the strongest stereochemical effects and these have been observed in free-radical additions to alkenes, as well as elimination from and substitution in alkyl derivatives. The problem is largely associated with the β-substituted alkyl radical I formed as an intermediate in these reactions.

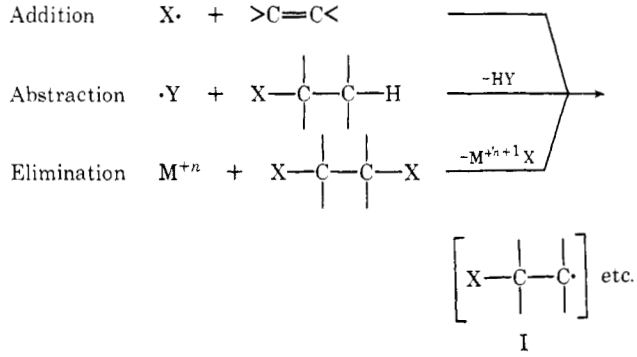

I

The β-bromo alkyl radical (I, X = Br) has been presented as a bridged species II and a similar delocalized structure has been attributed to the β-mercaptoalkyl radical III.[1]

II III

The electron spin resonance (esr) spectra of these radicals would provide the most direct approach to the study of their structure. In this paper we present an esr study of two groups of alkyl radicals substituted in the β position with an alkylmercapto group (IV) or a group IV metal (V). The esr spectra of these two

IV R = alkyl

V R = H, CH_3, CH_3CH_2, etc. M = Si, Ge, Sn

classes of β-substituted alkyl radicals show remarkable similarities but they are unique compared to their hydrocarbon analogs. In the following presentation the esr spectra of a series of free radicals IV and V are

(1) P. S. Skell, *Chem. Soc., Spec. Publ.*, No. 19, 131 (1965).

described first. The spectra are then interpreted in terms of radical structures involving preferential orientation of the heteroatom in the β position relative to the free-radical center. The latter implies incipient (p–d) interaction between the trigonal carbon atom and sulfur or the group IV metal.

Experimental Section

Esr spectra were taken with a modified Varian *X*-band spectrometer utilizing 100-kHz modulation. The microwave bridge was designed around a three-port ferrite circulator. A backward diode (Philco L4154B) was employed as detector in conjunction with a low-noise, wide-band preamplifier (Philco P301). The latter was provided with an impedance-matching input circuit and a simple dc circuit to monitor the crystal current by means of a sensitive galvanometer. The input transformer was wound in a ferrite pot core (Ferroxcube Inc.) and was carefully shielded with many layers of high magnetic permeability foil. A precision attenuator was placed before the tunable detector mount (Philco P955) and was used during tuning to avoid excessive microwave power on the detector.

The field of a 12-in. magnet was swept very linearly by a Varian V3506 magnet flux stabilizer equipped with a modified Varian V3507 slow-sweep unit. The spectral scans were accurately calibrated by means of a field marker operating in conjunction with a Harvey-Wells FC-502 nmr gaussmeter and a Hewlett-Packard frequency counter. The field marker caused the superposition of markers at accurately known field values directly onto the spectral record.

Briefly the field marker operates as follows. The field at the water sample of the nmr gaussmeter is modulated at 60 Hz by a pair of small coils. Therefore, when the resonance condition is exactly satisfied, the output of the instrument consists of a train of equidistant ringing patterns with a repetition rate of 120 Hz or twice the modulating frequency. This output is normally applied to the vertical plates of a monitor scope and is used for a field measurement. As the magnetic field moves in either direction from the center of the nmr absorption, the ringing patterns will no longer be equidistant from each other but will merge in pairs and will eventually disappear. This behavior can be utilized to monitor the condition of resonance by means of a coincidence circuit consisting of two channels. In the first channel, the ringing patterns are converted into short pulses coinciding with the leading edge of the resonance pattern. The second channel converts the 60-Hz line voltage into a train of short pulses with a repetition rate of 120 Hz. This channel also has a variable phase-shifting network. The two channels are the inputs to an "AND" gate which generates an output only when the two trains of pulses are exactly in coincidence. This condition prevails only at resonance if the pulses derived from the line voltage are in phase with the 60-Hz modulation at the water nmr probe. The output of the gate is then used to cause the superposition of a spike on the esr spectrum being recorded and to lock the frequency counter so that it displays the nmr frequency at resonance. In practice one initiates a magnetic scan with the nmr oscillator set for a frequency corresponding to a magnetic field value just ahead of the sweeping field. When the resonance condition is exactly satisfied a marker is superposed on the spectrum, and the nmr frequency displayed by the counter is recorded on the chart. The nmr oscillator is then advanced beyond the instantaneous value of the sweeping field for another marker. Each scan is thus indexed with a series of markers which can be used to measure the positions of the lines by interpolation between neighboring markers. More commonly, however, an average scale in kilohertz per centimeter is obtained which is used to convert into gauss (4.258 kHz/G) the splittings measured with a ruler. We consider the hyperfine splittings measured in this manner to be accurate within ± 0.03 G. The major source of error is the slow drift of the klystron microwave frequency during a scan.

The light source was a water-cooled 2-kW mercury discharge lamp (Pek Labs A-1-B) powered by a transformer and held in a water jacket assembly (Geo. W. Gates and Co., A154G14) with a Suprasil quartz (Amersil, Inc.) body. The lamp housing had a fan and a spherical mirror assembly with the lamp in its center of curvature. The optical system consisted of a condenser lens (1.5-in. diameter, 1.5-in. focal length, Suprasil quartz) with the lamp at its focal point, a cylindrical cooling cell (5 cm in length with Suprasil end plates) through which circulated a 0.1 *M* $NiCl_2 \cdot 6H_2O$ solution, a simple shutter, and a refocussing lens (1.5-in. diameter, 3.5-in. focal length) with the sample in the cavity at its focal point.

An unsilvered dewar system with flowing dry nitrogen cooled by passage through a heat exchanger was used to vary the temperature of the sample. The unsilvered tip of the dewar (6-mm id) which passed through the sensitive part of the cavity was made of Suprasil quartz. The latter does not develop spurious paramagnetic centers on prolonged irradiation and has a higher transmission in the far-uv than ordinary quartz. To increase the uv flux at the sample, the optical transmission end plate of a Varian V4531 rectangular cavity was replaced with a similar end plate with much wider slots (ten horizontal slots separated by as little metal as possible) without appreciable loss of *Q*. The exit of the dewar was flushed by dry air to avoid excessive condensation of moisture. The temperature of the sample was monitored by a thermocouple placed just below the sensitive part of the cavity. Because of the intense radiation from the mercury arc the temperature of the irradiated sample was several degrees higher than that monitored by the thermocouple. Periodically, this difference in temperature was measured by a second thermocouple. The latter was placed in a sample tube containing methyl alcohol and carefully positioned to be in the center of the cavity. The temperature difference between the two thermocouples was applied as a correction to the temperatures measured during actual photolysis experiments by the monitoring thermocouple. This correction amounted to 10–20° and was found to vary from lamp to lamp. We believe that the temperatures reported here are within, at most, 5° of the true temperature in the irradiated region of the sample.

Since most materials used in this study were of relatively low dielectric loss, it was advantageous to use cylindrical sample tubes of as wide an internal diameter as possible. The bottom parts of the sample tubes were made of 5-mm o.d. and 4-mm i.d. Suprasil tubing and were joined to Pyrex tubing *via* graded seals for ease of handling. The Pyrex part had a small bulb to facilitate mixing of the contents and a ground glass joint. Typically, a small amount of di-*tert*-butyl peroxide or alkyl disulfide (about $^1/_5$th of the final volume) was introduced in the tube followed by the desired amount of parent hydrocarbon or group IV hydride if liquids at room temperature. The contents of the tube were thoroughly degassed on a vacuum system by freeze–pump–thaw cycling after which the desired amount of diluent (cyclopropane, ethane), if needed, or the parent compound, if a gas at room temperature, was introduced into the sample tube by bulb-to-bulb distillation. The tube was then sealed off with a flame just above the bulb and the contents were stirred by repeatedly inverting the tube in a Dry Ice–acetone bath (or a colder bath if very low boiling materials were handled). With the tube upside down in the cold bath, a Teflon collet was slipped in place and the part of the tube to be inserted in the cavity was thoroughly cleaned and dried. Finally, the tube was removed from the cold bath, turned upright, and quickly inserted in the unsilvered dewar kept at an appropriate low temperature.

All compounds employed in this study were reagent grade commercial samples most of which were used without further purification. The di-*tert*-butyl peroxide was obtained from Wallace and Tiernan and was also used without further purification. Most of the disulfides, however, were passed over activated alumina (M. Woelm Co.) prior to use. This treatment was found to remove the slight yellow coloration of most commercial disulfides.

Results

The esr spectra of transient radicals in solution were examined by a general technique utilizing *tert*-butoxy radicals generated photochemically from di-*tert*-butyl peroxide directly in the cavity of the spectrometer.[2] In a similar manner, thiyl radicals were produced from the photolysis of a variety of dialkyl disulfides.[3] Neither

$$(CH_3)_3COOC(CH_3)_3 \xrightarrow[(2537\ \text{Å})]{h\nu} 2(CH_3)_3CO\cdot$$

(2) (a) P. J. Krusic and J. K. Kochi, *J. Amer. Chem. Soc.*, **90**, 7155 (1968); (b) see also R. O. C. Norman, Ed., *Chem. Soc., Spec. Publ.*, **No. 24**, 147 (1970).

(3) (a) R. M. Kellogg, *Methods Free-Radical Chem.*, **2**, 1 (1969); (b) Annual Reports on Mechanisms of Reactions of Sulfur Compounds, Vol. 2, Intra-Science Research Foundation, Santa Monica, Calif., 1968; (c) K. Griesbaum, *Angew. Chem., Int. Ed. Engl.*, **9**, 273 (1970).

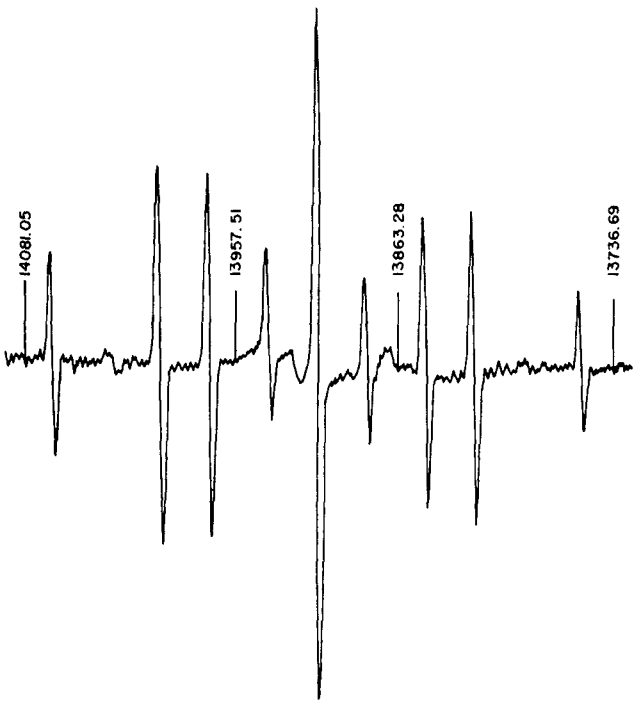

Figure 1. Esr spectrum of $CH_3SCH_2CH_2\cdot$ from the addition of methylthiyl radical to ethylene at −80°. The proton nmr field markers are in kilohertz.

the esr spectrum of the *tert*-butoxy radical nor that of

$$RSSR \xrightarrow{h\nu} 2RS\cdot$$

the thiyl radical was a complicating factor in these studies.

The Esr Spectra of β-Mercaptoalkyl Radicals. A series of β-mercaptoalkyl radicals VI were generated by photolysis of a solution of dialkyl disulfide in the presence of ethylene, propylene, isobutylene, and tetramethylethylene. The esr spectrum shown in Figure 1 for the methylmercaptoethyl radical generated from dimethyl disulfide and ethylene is typical of the quality obtainable. All of these spectra were readily interpreted on the basis of the alkene addendum; *i.e.*, the splitting consisted of a triplet of triplets from ethylene, a doublet of triplets of quartets from propylene, a

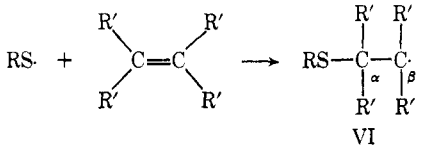

VI

R = CH_3, $(CH_3)_3C$, CF_3; R′ = H, CH_3

triplet of septets for isobutylene, and a broadened septet for tetramethylethylene with the usual binomial intensity distributions. The trifluoromethylmercapto adduct to ethylene showed, in addition, a significant quartet splitting due to three fluorine atoms. The hyperfine splitting due to the three hydrogens in the methylthiyl adduct was unresolved.

The magnitudes of the coupling constants listed in Table I of a variety of these β-mercaptoalkyl radicals are reasonably analogous to those of the corresponding hydrocarbon radicals with two important exceptions. The hyperfine splitting due to the β protons (in the methylene group attached to sulfur) is significantly smaller (13–17 G) than is that usually encountered in acyclic hydrocarbon radicals (23–35 G). The β-coupling constants for these protons also show marked temperature dependence in contrast to the others.

Table I. Hyperfine Coupling Constants for β-Mercaptoalkyl Radicals VI by Addition of Thiyl Radicals to Alkenes[a]

Thiyl radical[a]	Alkene	Temp, °C	Coupling constant, G a_α	a_β	a_{CH_3}
$CH_3S\cdot$	$CH_2{=}CH_2$	−70	21.60	14.89	
		−124	21.68	13.50	
$(CH_3)_3CS\cdot$	$CH_2{=}CH_2$	−73	21.65	16.87	
		−110	21.65	15.97	
$CF_3S\cdot$	$CH_2{=}CH_2$	−83	22.03	13.82	4.34[b]
		−127	21.96	12.81	4.42[b]
		−162	21.82	11.89	4.47[b]
$CH_3S\cdot$	$CH_2{=}CHCH_3$	−30	21.26	13.89	24.25
		−81	21.36	12.94	24.13
$(CH_3)_3CS\cdot$	$CH_2{=}CHCH_3$	−84	21.38	13.81	24.10
		−133	21.45	12.68	24.08
$CH_3S\cdot$	$CH_2{=}C(CH_3)_2$	+26		12.82	22.84
		−84		11.20	22.37
$CH_3S\cdot$	$(CH_3)_2C{=}C(CH_3)_2$	−54		*c*	22.45

[a] Hyperfine splitting due to alkylmercapto group unresolved. [b] Quartet splitting due to trifluoromethyl group. [c] γ-Hydrogens (methyl) unresolved.

The adduct VII of methylthiyl radical and allyl methyl sulfide places both methylene groups adjacent to a sulfur atom. The esr spectrum of VII consisted simply of a doublet of quintets showing *both methylene groups to be equivalent*. The magnitudes of the coupling

$$CH_3S\cdot + CH_2{=}CHCH_2SCH_3 \longrightarrow \underset{\text{VII}}{CH_3SCH_2\dot{C}HCH_2SCH_3}$$

constants are also consistent with the series of β-mercaptoalkyl radicals presented in Table I (a_α = 20.99 and 21.15 G, a_β = 15.42 and 14.64 G at +10 and −41°, respectively).

The esr spectrum of the allylic radical VIII produced by *addition* of thiyl radicals to 1,3-butadiene in the s-trans conformation is shown in Figure 2. The

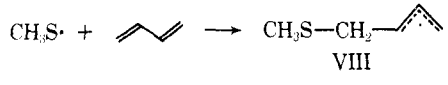

VIII

hyperfine coupling constants listed in Table II for this

Table II. Hyperfine Coupling Constants for Substituted *trans*-α-Methallyl Radicals

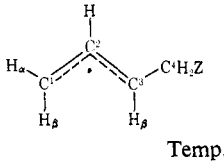

Z =	Temp, °C	Hyperfine coupling constants, G[a] $H_{1\alpha}$	$H_{1\beta}$	H_2	$H_{3\beta}$	H_4
		(d)	(t)	(d)	(t)	(q)
H	−110	14.78	13.83	3.85	13.83	16.43
		(d)	(d)	(d)	(d)	(t)
CH_3	−133	14.85	13.89	3.85	13.58	14.18
		(d)	(t)	(d)	(t)	(t)
$(CH_3)_3CO$	−67	14.68	13.60	3.93	13.60	16.47
	−127	14.83	13.74	3.88	13.74	16.97
		(d)	(d)	(d)	(d)	(t)
CH_3S	−66	14.51	13.53	3.81	13.26	9.20
	−105	14.47	13.53	3.75	13.24	8.75

[a] Letters in parentheses indicate splittings: d = doublet, t = triplet, q = quartet.

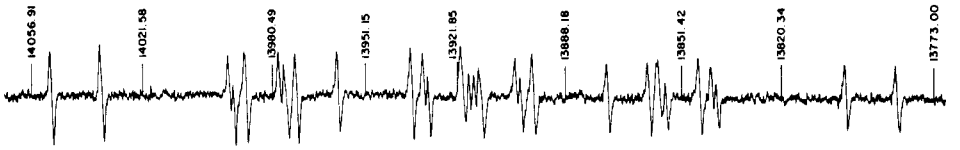

Figure 2. Esr spectrum of CH_3SCH_2—CH=CH—CH_2 from the addition of methylthiyl radical to butadiene at −120°. The $M_I = 0$ lines for the protons at C-4 are broadened beyond detection at this temperature (see text).

species are compared with a similar species derived from *tert*-butoxy radical as well as the parent hydrocarbon radical (*trans*-α-methallyl).

Table III. The Hyperfine Splitting Constants of the β Group IVb Analogs of *n*-Propyl Radical

Radical	Coupling constant, G a_α	a_β	a_γ	Temp, °C
$H_3CCH_2CH_2\cdot$	22.14	30.33	0.27	−110
$H_3SiCH_2CH_2\cdot$	21.39	17.68	2.77	−70
$H_3GeCH_2CH_2\cdot$	20.96	15.84	4.32	−80

The phenyl analog X can also be prepared from phenylsilane under similar conditions. In the esr spectrum taken at −97° the three pairs of α, β, and γ

$$PhSiH_2\cdot + CH_2{=}CH_2 \longrightarrow PhSiH_2CH_2CH_2\cdot \quad (X)$$

protons show up as triplets of 21.20, 17.72, and 1.71 G splitting, respectively. The hyperfine coupling constants of a variety of other aryl derivatives of β-silylalkyl radicals (generated in an analogous manner) are listed in Table IV.

Table IV. Hyperfine Coupling Constants for Phenyl Derivatives of β-Silylalkyl Radicals

Silane	Alkene	Radical	Temp, °C	Coupling constants, G a_α	a_β	a_{SiH}	a_{CH_3}
$PhSiH_3$	$CH_2{=}CH_2$	$PhSiH_2CH_2CH_2\cdot$	−65	21.20	17.72	1.71	
Ph_2SiH_2	$CH_2{=}CH_2$	$Ph_2SiHCH_2CH_2\cdot$	−87	21.08	17.79	0.66	
Ph_3SiH	$CH_2{=}CH_2$	$Ph_3SiCH_2CH_2\cdot$	−60	21.24	18.64		
Ph_3SiH	$CH_2{=}C(CH_3)_2$	$Ph_3SiCH_2\dot{C}(CH_3)_2$[a]	−90		15.75		22.45

[a] In addition to 2-methallyl radical.

A comparison of these coupling constants shows that the hydrogen atoms attached directly to the allylic moiety, *i.e.*, $H_{1\alpha}$, $H_{1\beta}$, H_2, and $H_{3\beta}$ (Table II) are relatively insensitive to the substituent placed at C-4. A sulfur substituent, however, does sufficiently perturb the allylic portion of the radical to disrupt the degeneracy of $a_{1\beta}$ and $a_{3\beta}$ from a single triplet in *trans*-α-methallyl radical (and its *tert*-butoxy derivative) and alter the splitting to a pair of similar doublets. However, the most striking change effected by a sulfur substituent is at H-4. The triplet splitting associated with the methylene protons is small (~9 G). Furthermore, the central lines of the triplets are broadened to a point where they are barely observed at temperatures less than −80°. At a temperature close to 0° these triplets approach the expected 1:2:1 binomial intensity distribution.

The Esr Spectra of Alkyl Radicals β Substituted with Group IV Metals. A variety of methods were employed to generate alkyl radicals substituted with group IV metals. These are described individually below.

Silicon. The esr spectrum of β-silylethyl radical IX was obtained from the photolysis of a solution of silane and di-*tert*-butyl peroxide in ethylene. The radical species is identified as the β-silylethyl radical IX.

$$SiH_4 + (CH_3)_3CO\cdot \longrightarrow \cdot SiH_3 + (CH_3)_3COH$$

$$H_3Si\cdot + CH_2{=}CH_2 \longrightarrow H_3SiCH_2CH_2\cdot \quad (IX)$$

The coupling constants are compared with those from the analogous hydrocarbon species in Table III. Under these conditions the esr spectrum of the silyl radicals was not observed.

The triethyl derivative XI was generated from triethylsilane and di-*tert*-butyl peroxide in ethylene (Table V). Photolysis of tetraethylsilane and di-*tert*-butyl

$$(CH_3CH_2)_3SiH + (CH_3)_3CO\cdot \longrightarrow (CH_3CH_2)_3Si\cdot + (CH_3)_3COH$$

$$(CH_3CH_2)_3Si\cdot + CH_2{=}CH_2 \longrightarrow (CH_3CH_2)_3SiCH_2CH_2\cdot \quad (XI)$$

peroxide in cyclopropane solutions also generated XI in addition to the isomeric XII. The esr spectra of the

$$(CH_3CH_2)_3SiCH_2CH_3 + (CH_3)_3CO\cdot \begin{cases} \longrightarrow (CH_3CH_2)_3SiCH_2CH_2\cdot & XI \\ \longrightarrow (CH_3CH_2)_3Si\dot{C}HCH_3 & XII \end{cases}$$

α-silylalkyl radicals XII have been discussed previously.[4] Although the γ-hydrogens (methylene) were unresolved in XI, the values for the α and β coupling constants were similar to other radicals presented above.

The triethylsilyl radical also added to isobutylene under these conditions to generate the tertiary radical XIII. The esr spectrum shown in Figure 3 consisted simply of a septet (22.5 G) split further into triplets (15.35 G). The γ-hyperfine coupling constants were unresolved.

$$(CH_3CH_2)_3Si\cdot + CH_2{=}C(CH_3)_2 \longrightarrow (CH_3CH_2)_3SiCH_2\dot{C}(CH_3)_2 \quad (XIII)$$

(4) P. J. Krusic and J. K. Kochi, *J. Amer. Chem. Soc.*, 91, 6161 (1969).

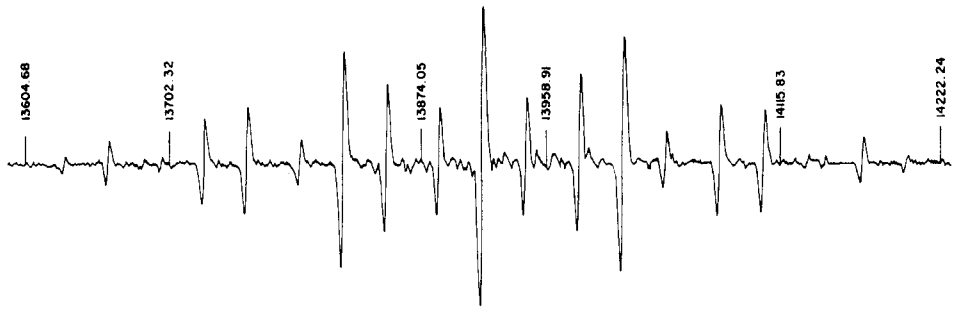

Figure 3. Esr spectrum of $(C_2H_5)_3SiCH_2\dot{C}(CH_3)_2$ from the addition of triethylsilyl radicals to isobutylene at $-111°$.

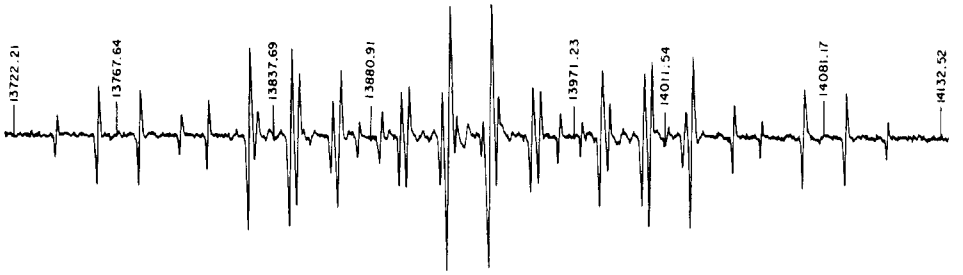

Figure 4. Esr spectrum of $H_3GeCH_2CH_2\cdot$ from the addition of germyl radicals to ethylene at $-118°$.

Germanium. The direct photolysis of a solution of germane and di-*tert*-butyl peroxide in ethylene at $-119°$ led to the esr spectrum shown in Figure 4. The spectrum

$$GeH_4 + (CH_3)_3CO\cdot \longrightarrow H_3Ge\cdot + (CH_3)_3COH$$

$$H_3Ge\cdot + CH_2{=}CH_2 \longrightarrow \underset{\text{XIV}}{H_3GeCH_2CH_2\cdot}$$

can be unambiguously assigned to the adduct radical XIV in which the α, β, and γ coupling constants are 20.96, 15.84, and 4.32 G, respectively (Table III). The intensity of this spectrum is in contrast to the poor quality of that of the germyl radical $GeH_3\cdot$ obtained in the absence of ethylene. The latter may be attributed to the greater stability of XIV compared to $GeH_3\cdot$.

The photolysis of a solution of tetraethylgermane and di-*tert*-butyl peroxide in cyclopropane solution led to a mixture of two isomeric radicals XV and XVI. The esr spectrum of the latter has been discussed earlier.[4] The radical species XV (triplet of triplets) had a slightly

$(CH_3CH_2)_4GeCH_2CH_3$ +

$$(CH_3)_3CO\cdot \longrightarrow \begin{cases} (CH_3CH_2)_3GeCH_2CH_2\cdot & \text{XV} \\ (CH_3CH_2)_3Ge\dot{C}HCH_3 & \text{XVI} \end{cases}$$

larger g value (Δg = 0.00054) than XVI (doublet of quartets) and it is the minor component of the spectrum (Table V).

Table V. Hyperfine Coupling Constants for β-Silyl-, β-Germyl-, and β-Stannylalkyl Radicals

Radical $R_3MCH_2CH_2\cdot$	Temp, °C	Coupling constant, G a_α	a_β	a_{CH_3}
$(CH_3CH_2)_3SiCH_2CH_2\cdot$	−119	21.01	17.67	
$(CH_3CH_2)_3SiCH_2\dot{C}HCH_3$	−101	21.10	16.74	24.26
$(CH_3CH_2)_3SiCH_2\dot{C}(CH_3)_2$	−101		15.35	22.25
$(CH_3CH_2)_3GeCH_2CH_2\cdot$	−118	20.70	16.42	
$(n\text{-}C_4H_9)_3SnCH_2CH_2\cdot$	−148	19.64	15.67	

Tin. Alkyl radicals substituted in the β position with the tin moiety were also readily generated by addition of stannyl radicals to alkenes. Thus, photolysis of a solution of tri-*n*-butylstannane and di-*tert*-butyl peroxide in ethylene generated the adduct XVII. The

$$Bu_3SnH + (CH_3)_3CO\cdot \longrightarrow Bu_3Sn\cdot + (CH_3)_3COH$$

$$Bu_3Sn\cdot + CH_2{=}CH_2 \longrightarrow \underset{\text{XVII}}{Bu_3SnCH_2CH_2\cdot}$$

coupling constants in this radical (a_α = 19.64 G, a_β = 15.67 G, $T = -148°$) are significantly smaller than corresponding values in the germanium and silicon analogs (Table V). The triethyl analog of XVII was also produced by photolysis of di-*tert*-butyl peroxide in the presence of tetraethylstannane. The isomeric α-substituted radical XVIII was the predominant species as it was with tetraethylgermane.

$$(CH_3CH_2)_4Sn + (CH_3)_3CO\cdot \longrightarrow \begin{cases} (CH_3CH_2)_3Sn\dot{C}HCH_3 & \text{XVIII} \\ (CH_3CH_2)_3SnCH_2CH_2\cdot & \text{XVII} \end{cases}$$

Trimethylstannyl radicals generated by direct photolysis of hexamethyldistannane also add to ethylene. The coupling constants observed for the adduct radical

$$(CH_3)_3SnSn(CH_3)_3 \xrightarrow{h\nu} 2(CH_3)_3Sn\cdot$$

$$(CH_3)_3Sn\cdot + CH_2{=}CH_2 \longrightarrow \underset{\text{XIX}}{(CH_3)_3SnCH_2CH_2\cdot}$$

XIX (a_α = 19.74 G, a_β = 15.75 G at $-133°$) are consistent with those obtained for other β-stannyl radicals.

The Esr Spectra of β-Alkoxyalkyl Radicals. The esr spectra of a variety of β-oxy-substituted alkyl radicals were also studied in order to compare the conformations of these radicals with those found in the alkylmercapto and group IV substituted analogs.

The spectrum of the β-hydroxyethyl radical (Table VI) was observed as the minor species during photolysis

Table VI. Coupling Constants of β-Oxyalkyl Radicals

Radical	Temp, °C	Coupling constant, G a_α	a_β	a_{CF_3}
$HOCH_2CH_2\cdot$ [a]	−71	22.00	31.67	
$CH_3OCH_2CH_2\cdot$	−41	22.08	31.45	[b]
$CF_3OCH_2CH_2\cdot$	−74	22.73	28.72	2.00

[a] Taken from ref 5. [b] a_{CH_3} (unresolved) < 0.1 G.

of a stationary solution of hydrogen peroxide in ethyl alcohol and compares with the results of Livingston and Zeldes in flow systems.[5] The *tert*-butoxy radicals generated in a similar manner from di-*tert*-butyl peroxide only gave rise to the more stable α-hydroxyethyl radical.

$$HO\cdot + CH_3CH_2OH \begin{cases} \longrightarrow CH_3\dot{C}HOH + H_2O \\ \longrightarrow \cdot CH_2CH_2OH + H_2O \end{cases}$$

The β-methoxyethyl radical was produced by photolysis of β-methoxypropionyl peroxide in cyclopropane solution.[6] In addition to the major species we also

$$CH_3OCH_2CH_2{-}\overset{O}{\overset{\|}{C}}{-}O{-}O{-}\overset{O}{\overset{\|}{C}}{-}CH_2CH_2OCH_3 \longrightarrow 2CH_3OCH_2CH_2\cdot + 2CO_2$$

observed the spectrum of a minor component consisting of a triplet (a_α = 17.15 G) of triplets (a_γ = 2.21 G) of slightly higher g value. We assign this spectrum to the isomeric ethoxymethyl radical[7] which may be formed *via* an intramolecular rearrangement or by induced decomposition of the peroxide.

$$CH_3OCH_2CH_2\cdot \longrightarrow \cdot CH_2OCH_2CH_3$$

The β-trifluoromethoxyethyl radical was generated by photolysis of a solution of ethylene in bistrifluoromethyl peroxide. Under the same conditions we were

$$CF_3O\cdot + CH_2{=}CH_2 \longrightarrow CF_3OCH_2CH_2\cdot$$

unable to observe the addition of *tert*-butoxy radicals to ethylene. A sizable hyperfine coupling to the three fluorine atoms was observed (Table VI) while the corresponding methyl hydrogens in methoxyethyl radical gave no resolvable structure. It should be noted that the magnitude of the fluorine coupling constant in the sulfur radical (Table I) is approximately twice that of the oxygen analog. All of the radicals listed in Table VI have in common β coupling constants which are of comparable magnitude to those found in *n*-propyl and *n*-butyl radicals[6] and they show similar temperature dependences.

Discussion

Alkyl radicals with sulfur, silicon, germanium, or tin substituted in the β position all exhibit characteristic and unique esr spectra compared to their hydrocarbon analogs. Furthermore, the presence of an oxygen or nitrogen atom in the β position of alkyl radicals does not induce an effect of comparable magnitude.[5,8] Any interpretation of the spectra relative to the structure of these group IV or sulfur-substituted alkyl radicals must take into account the following observations: (a) an unusually small value for the coupling constants associated with β-hydrogens attached to the carbon atom bearing the heteroatom (S, Si, Ge, Sn); (b) the relatively large temperature coefficients which are uniquely associated with these coupling constants; (c) the otherwise expected values of the coupling constants for all other β-hydrogens; (d) the large value of the γ coupling constant in β-silyl, -germyl, and -stannylethyl radicals; (e) substantially larger β-coupling constants for β-*tert*-butylthiyl alkyl radicals compared to their β-methylthiyl counterparts; (f) the large value of the fluorine coupling constant in β-trifluoromethyl mercaptoalkyl radicals and marked temperature-dependent line broadening effects on the spectrum; (g) the observation of splitting by the hydrogen atoms at C-4 in α-mercaptomethylallyl radical VIII, which is approximately half that of the oxygen and carbon analogs.

In the following analysis we examine the variation in the isotropic hyperfine coupling constants of β-hydrogens in alkyl radicals with the rotational conformation about the α,β bond. The temperature dependence of the coupling constants is then examined relative to the barrier to internal rotation from the most stable configuration.

Theoretical Considerations. The isotropic hyperfine coupling constant of a β-hydrogen in an alkyl radical depends strongly on its orientation relative to the free-radical center. The angular dependence of a_β can be approximated by eq 1, where θ is the dihedral angle

$$a_\beta = A + B\cos^2\theta \qquad (1)$$

between the β carbon–hydrogen bond and the axis of the trigonal-carbon atom. The equation is consistent with the hyperconjugative mechanism proposed for β interactions. It is also predicted by SCF–MO–LCAO calculations using the semiempirical INDO approximation (*vide infra*).

For a radical in solution there will be a rotational motion about the C_α–C_β bond which will generally be under the influence of a periodic potential. In each trough of the potential function the radical will exist in a number of torsional states followed by rotational states above the barrier. A change in the state of the motion can occur in any of the following ways: transitions between torsional states, excitation to a rotational level above the barrier followed by a classical rotation, or tunneling through the barrier. The correlation times for the first type of motion are much shorter than the time scale of the esr experiment. The observed esr spectrum, therefore, shows a β-proton coupling constant which is an average over the torsional states. The reciprocal of the correlation times for the remaining two types of motions however may be comparable in magnitude to differences in hyperfine frequencies and selective broadening of the lines may occur.

The theory of quantum-mechanical averaging of the β-proton coupling constant in the presence of a twofold

(5) R. Livingston and H. Zeldes, *J. Chem. Phys.*, **44**, 1245 (1966).
(6) J. K. Kochi and P. J. Krusic, *J. Amer. Chem. Soc.*, **91**, 3940 (1969).
(7) Compare with the α-hydroxy and α-alkoxy radicals derived from alcohols and ethers. See ref 5 and W. T. Dixon, R. O. C. Norman, and A. Buley, *J. Chem. Soc.*, 3625 (1964); T. Shiga, A. Boukhors, and P. Douzou, *J. Phys. Chem.*, **71**, 3559 (1967); A. Hudson and K. D. J. Root, *Tetrahedron*, **25**, 5311 (1969).
(8) W. E. Griffiths, G. F. Longster, J. Myatt, and P. F. Todd, *J. Chem. Soc. B*, 530 (1967).

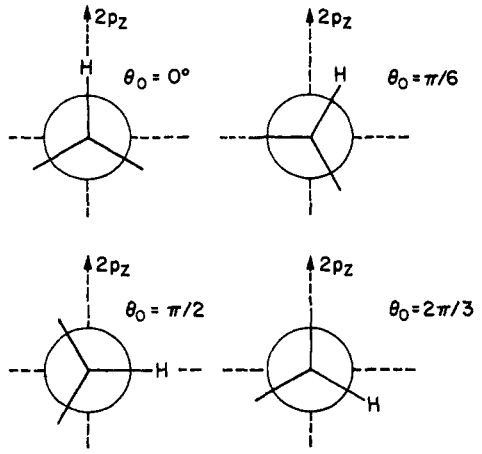

Figure 5. Equilibrium conformations for β protons in alkyl radicals.

sinusoidal potential (eq 2) has been treated with a

$$V_2(\alpha) = \frac{V_0}{2}(1 - \cos 2\alpha) \tag{2}$$

number of approximations by Stone and Maki[9] and more rigorously by Fessenden.[10] The problem consists of calculating the expectation value of $\cos^2\theta$ for the ith torsional state, $\langle i|\cos^2\theta|i\rangle$, in the representation which diagonalizes the torsional Hamiltonian where $I = I_aI_b/(I_a + I_b)$ represents the reduced moment of

$$\mathcal{H} = -\left(\frac{h^2}{2I}\right)\frac{\partial^2}{\partial\alpha^2} + V_2(\alpha) \tag{3}$$

inertia relative to the moments of inertia I_a and I_b of the two rotating groups. The β coupling constant for the radical in the ith torsional state will then be $\langle a_\beta\rangle_i = A + B\langle i|\cos^2\theta|i\rangle$. The observed coupling constant is the Boltzman-weighted average of these values, and is given by eq 4, in which E_i is the energy

$$\langle a_\beta\rangle = \frac{\sum_{i=0}^{\infty}\langle a_\beta\rangle_i \exp(-E_i/kT)}{\sum_{i=0}^{\infty}\exp(-E_i/kT)} \tag{4}$$

of the ith torsional state. In the limiting case of free rotation (a situation approximated by the ethyl radical and generally by methyl groups attached to the α-carbon atom) eq 4 reduces to eq 5. All alkyl radicals pre-

$$a_\beta = A + {}^1/_2B \tag{5}$$

sumably approach the limit imposed by eq 5 at high temperatures.

Fesseden[10] has successfully applied this approach to a number of alkyl radicals such as isobutyl, *n*-propyl, 3-butenyl, and deuterated ethyl radicals. He has explained cases where the β coupling constants depart from the "free rotation" limit and has derived values for the heights of the potential barriers from the temperature dependence of the β coupling constants.

In addition to the approximate quantum mechanical treatment, Stone and Maki[9] have also discussed the averaging of the $\cos^2\theta$ dependence (eq 1) from a classical point of view. In this approach the alkyl group is assumed to execute a classical oscillatory motion about its equilibrium conformation under the influence of a quadratic potential. This treatment is intrinsically incapable of yielding the heights of the potential barriers and involves, furthermore, a type of motion which is much too localized for the barriers to internal rotation of the magnitude considered here. One can indeed estimate the frequency of transitions *via* classical rotation from one trough of the potential function to the adjacent one by eq 6. For a primary alkyl radical ($I_{eff} \approx 2.9 \times 10^{-40}$ g cm^2) with $V_0 = 1000$ cal/mol, one calculates a frequency of 5.5×10^{11} sec^{-1} at room

$$\omega_r = \frac{1}{\pi}\left[\frac{V_0}{2I_{eff}}\right]^{1/2} e^{-V_0/kT} \tag{6}$$

temperature. With such frequencies a model involving localized torsional oscillation even of considerable amplitude is obviously not realistic.

An alternative approach is to consider the classical limit to which eq 4 tends as the reduced moment of inertia increases. The separation between torsional states ΔE_i diminishes and a continuum is approached when all the values of the potential function become allowed. The classical limit of eq 4 is then given by eq 7, where $V(\theta)$ is the twofold sinusoidal potential

$$\langle a_\beta\rangle = \frac{\int_{-\pi}^{\pi} a_\beta(\theta)\exp(-V(\theta)/kT)d\theta}{\int_{-\pi}^{\pi}\exp(-V(\theta)/kT)d\theta} \tag{7}$$

represented in eq 2 and $a_\beta(\theta)$ is the angular dependence of the coupling constant (eq 1). This expression can be handled conveniently by digital computers. It simply represents the anisotropic averaging of the $\cos^2\theta$ dependence using as a statistical weight the Boltzman probability that the radical may be found in a state with a torsional energy $V(\theta)$ and, therefore, with an angle of twist θ. If we always measure this angle θ from the p_z axis of the trigonal carbon we need consider only four cases (illustrated in Figure 5) which represent the conformations commonly encountered at the potential minima. The classical anisotropic averages of the β coupling constants for the proton in the four conformations given in Figure 5 are then given by eq 7 with

$$a_\beta^{(i)}(\theta) = A + B\cos^2(\theta + \theta_0^{(i)}) \tag{8}$$

We apply the foregoing classical theory to the primary alkyl radicals considered earlier by Fessenden.[10] The temperature dependence of the β coupling constants for the isobutyl, *n*-propyl, and 3-butenyl radicals obtained by Fessenden are shown in Figure 6. In all cases the β coupling constants are considerably higher than the "free rotation" limit of 26.87 G, although the latter is approached with increasing temperatures. The large magnitudes of a_β for the isobutyl radical led Fessenden to assign to it the equilibrium conformation in which the single β proton is eclipsed by the p orbital ($\theta_0 = 0$, Figure 5). The somewhat reduced magnitudes of the β couplings and the *equivalence* of the pair of β protons of the *n*-propyl and 3-butenyl radicals at all

(9) E. W. Stone and A. H. Maki, *J. Chem. Phys.*, 37, 1326 (1962).
(10) R. W. Fessenden, *J. Chim. Phys. Physicochim. Biol.*, 61, 1570 (1964).

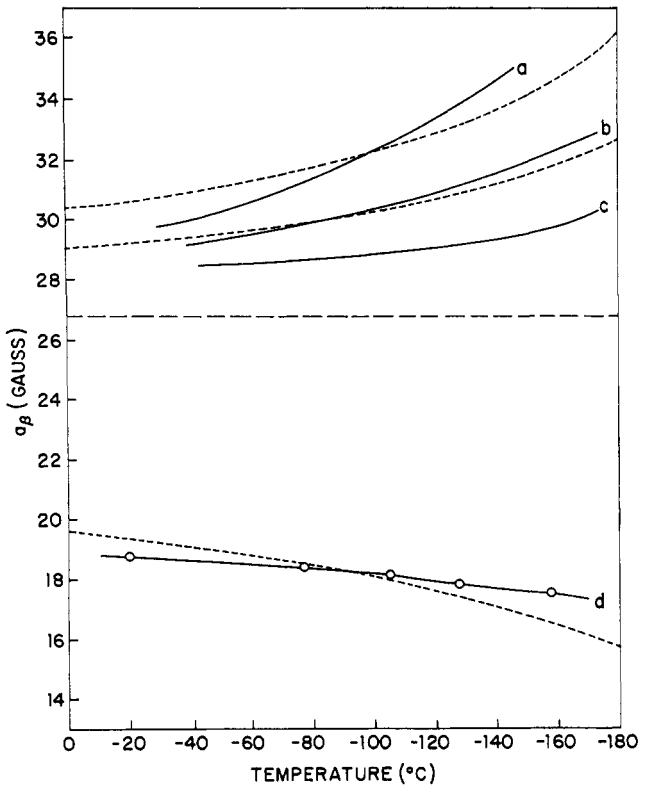

Figure 6. Upper: experimental temperature dependence of β coupling constants for (a) isobutyl, (b) *n*-propyl, and (c) allylcarbinyl radicals (after Fessenden[10]). Lower: (d) *tert*-amyl radical. Dotted lines are calculated (see text).

mechanical treatment (Figure 6). Convergence in these calculations is rapid and independent of the starting value for V_0. The barrier heights corresponding to the three curves are 300 cal/mol for isobutyl, 420 cal/mol for *n*-propyl, and 230 cal/mol for 3-butenyl in excellent agreement with Fessenden's values. We conclude, therefore, that the classical theory is quite adequate in treating the effects of rotational averaging of the $\cos^2\theta$ dependence for reduced moments of inertia and barrier heights of the magnitude considered here.

We have carried out similar iterative least-squares calculations varying both V_0 and B in an effort to determine both parameters from experimental data. Convergence, however, was not always obtained and we feel that these results may be questionable.

We have also examined the temperature dependence of a_β for isobutyl, *n*-propyl, and 3-butenyl radicals and confirm the equilibrium conformation deduced by Fessenden. Thus, the esr spectra of both the *n*-propyl (Figure 7) and 3-butenyl (Figure 8) radicals exhibit a temperature-dependent line broadening of the lines corresponding to $M = 0$ for the α protons. The esr spectrum of the isobutyl radical shows no line-width alternation over the same temperature range. This line-width effect is also a consequence of hindered rotation and it implies excursions between the troughs of the twofold potential at a rate (eq 6) which is comparable to the difference in the hyperfine frequencies for the α protons. The latter must, therefore, be magnetically inequivalent while the β protons remain

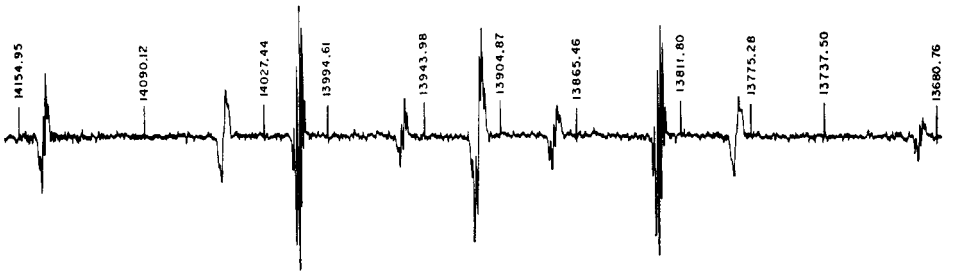

Figure 7. Esr spectrum of *n*-propyl radical from the photolysis of *n*-butyryl peroxide in cyclopropane solution at −140°, showing second-order splittings (third multiplet from each end of the spectrum) and line-width effect.

temperatures suggested the equilibrium conformation with $\theta_0 = \pi/6$ for these radicals.

The calculated curves for a_β obtained by the quantum mechanical approach employed by Fessenden are also reproduced in Figure 6. He calculated these values of a_β using eq 4 and assuming $A = 0$ and $B = 2 \times 26.87$ for the constants in eq 1. The heights of the potential barriers, V_0, employed in these calculations to obtain the best agreement were 295 cal/mol for isobutyl, 412 cal/mol for *n*-propyl, and 223 cal/mol for the 3-butenyl radical.

We have calculated the temperature dependences of a_β for the same radicals using the same values of A and B and employing the classical anisotropic averaging given by eq 7 as a function of the barrier height. The phases employed in eq 8 were $\theta_0 = 0$ for isobutyl and $\theta_0 = \pi/6$ for *n*-propyl and 3-butenyl radicals. The best fits to Fessenden's experimental points using a least-squares Newton–Raphson iterative procedure are nearly coincident with those obtained by the quantum equivalent in the two potential minima. These observations require that the phase be $\theta_0 = \pi/6$ (Figure 5). The absence of any line broadening for the isobutyl radical, on the other hand, clearly demands the symmetric conformation consistent with the phase $\theta_0 = 0$.

Heretofore, we have considered only primary alkyl radicals $RCH_2\cdot$ for which we have assumed (following Fessenden) that $A = 0$, and B was related to $a_\beta^{CH_3}$ for the ethyl radical according to eq 5. We wish to consider next how A and B are modified when one or both α-hydrogen atoms of $RCH_2\cdot$ are replaced with methyl groups to obtain secondary and tertiary alkyl radicals, respectively. In analogy with primary alkyl radicals, A is again assumed to be negligible. The value of B is obtained (eq 5) from the observed splittings of the methyl protons, $a_\beta^{CH_3}$. For example, in the *sec*-butyl radical,[2] $CH_3\dot{C}H-CH_2CH_3$, $a_\beta^{CH_3} = 24.6$ G and is temperature independent indicating essentially free rotation of the methyl group. For this radical, $B =$

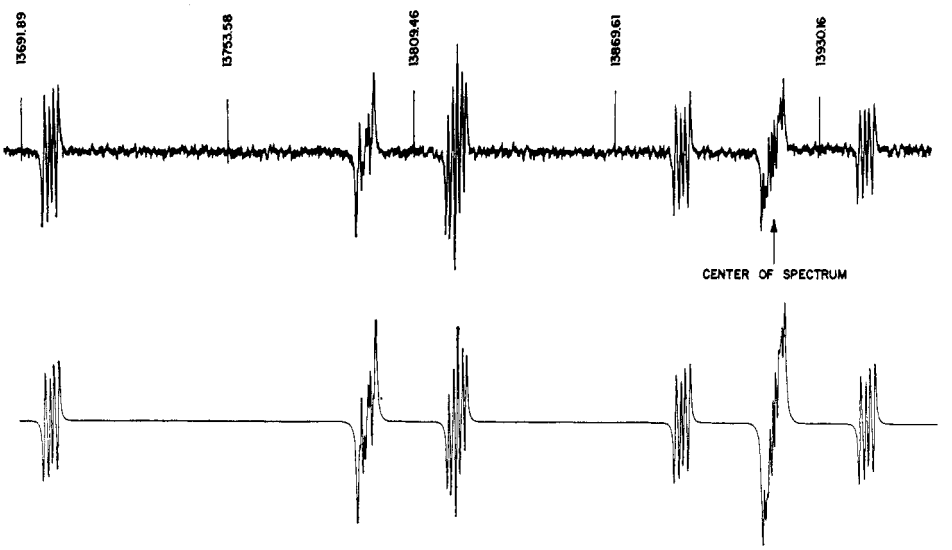

Figure 8. Experimental and calculated low-field halves of the esr spectrum of the alkylcarbinyl radical from the photolysis of allylacetyl peroxide in cyclopropane at −90°. The calculated spectrum includes second-order effects. A slightly larger line width for the lines corresponding to $M_1 = 0$ for the α protons was used in the computer simulation to achieve agreement with the experimental spectrum.

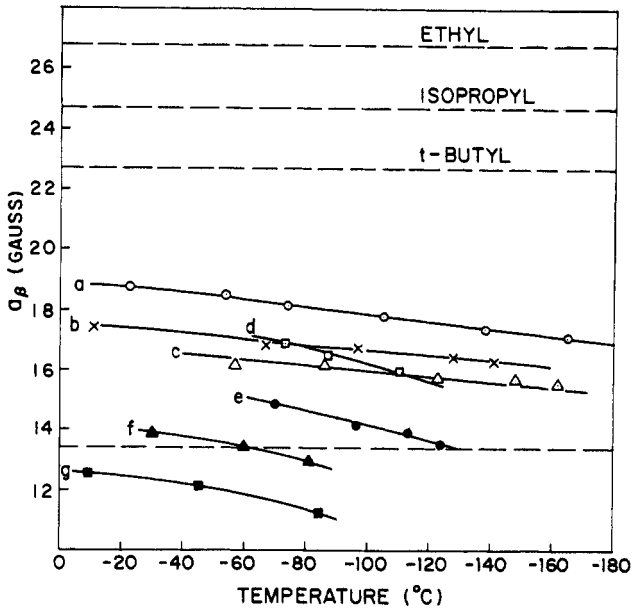

Figure 9. Experimental temperature dependence of the β coupling contants for: (a) $(C_2H_5)_3SiCH_2\dot{C}H_2$, (b) $(C_2H_5)_3GeCH_2\dot{C}H_2$, (c) $(n\text{-}C_4H_9)_3SnCH_2\dot{C}H_2$, (d) $(CH_3)_3CSCH_2\dot{C}H_2$, (e) $CH_3SCH_2\dot{C}H_2$, (f) $CH_3SCH_2\dot{C}HCH_3$, and (g) $CH_3SCH_2\dot{C}(CH_3)_2$. See text for dashed lines.

2 × 24.6 G. A more important example for our discussion is the *tert*-amyl radical, $(CH_3)_2\dot{C}CH_2CH_3$,[2] with $a_\beta^{CH_3}$ = 22.8 G which is also temperature independent. The value of B for this radical is therefore equal to 2 × 22.8 G. The splittings for the β-methylene protons $a_\beta^{CH_2}$ for the *tert*-amyl radical are *smaller* (~18 G) than the "free rotation" limit. Moreover, $a_\beta^{CH_2}$ is sensitive to changes in temperature and shows a positive temperature coefficient (Figure 6). The reduced magnitude of the β splittings and the equivalence (even at the lowest temperature studied) of the two methylene protons require the symmetric equilibrium conformation XX in which the γ-methyl group is eclipsed by the p orbital of the trigonal carbon atom. The angular dependence of the β couplings (CH_2) is then given by eq 8 with a phase $\theta_0 = 2\pi/3$ (Figure 5) and B = 45.6 G. Also shown in Figure 6 is the calculated temperature dependence using the classical anisotropic averaging formula (eq 7) with V_0 = 700 cal/mol. The agreement is as satisfactory here as it was

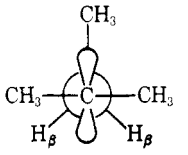

XX

with the primary radicals considered above. Indeed the classical approach should be even more appropriate in this case since the moments of inertia are now considerably larger. However, the theory fails to reproduce the slope of the experimental curve even in this favorable example. We shall return to a discussion of this problem again.

Conformations of Alkyl Radicals β Substituted with Group IV Elements and Sulfur. The alkyl radicals substituted in the β position with alkylmercapto, trialkylsilyl, trialkylgermyl, and trialkylstannyl groups (Tables I, III, IV, and V) *all* have in common unusually low values of β coupling constants (11–18 G) which show large temperature dependences. In Figure 9 the experimental curves are shown for the temperature dependence of the β coupling constants ($a_\beta^{CH_2}$) of the following representative radicals: $(C_2H_5)_3SiCH_2\dot{C}H_2$, $(C_2H_5)_3GeCH_2\dot{C}H_2$, $(n\text{-}C_4H_9)_3SnCH_2\dot{C}H_2$, $(CH_3)_3CSCH_2\dot{C}H_2$, $CH_3SCH_2\dot{C}H_2$, $CH_3SCH_2\dot{C}HCH_3$, and $CH_3SCH_2\dot{C}(CH_3)_2$. The values for the curve (a) at the three highest temperatures were obtained by hydrogen abstraction from tetraethylsilane. At the lower temperatures the radical was generated by addition of the triethylsilyl radical to ethylene. The points in curve b were obtained exclusively by hydrogen abstraction from tetraethylgermane. The organotin radicals (c) were generated by addition of tri-*n*-butylstannyl radicals to ethylene. Finally the three methylthioalkyl radicals were produced by addition of methylthiyl radicals to ethylene, propylene, and

isobutylene. Also shown in Figure 9 are the temperature-independent CH_3 coupling constants for ethyl, isopropyl, and *tert*-butyl radicals. These CH_3 coupling constants represent the approximate high-temperature limits for typical primary, secondary, and tertiary hydrocarbon radicals, respectively. The lowest dashed line in Figure 9 was drawn at $a_\beta = {}^1/_4B_{ethyl} = (0.5)(26.87\ G)$ and corresponds to the coupling constant which would be observed for the two equivalent β protons with $\theta_0 = \pm 2\pi/3$ (Figure 5) in a "frozen" ethyl radical (assuming $A = 0$). It constitutes, thus, a measure of the low-temperature limit for the β splittings in primary alkyl radicals.

From the results of the previous section it is clear that the behavior of the β splittings for these radicals is indicative of the symmetric equilibrium conformations XXI. In this conformation the heteroatom X is eclipsed by the p orbital of the radical center ($\theta_0 = 2\pi/3$). The proximity of the heteroatom X to the p orbital in conformation XXI is also supported by the larger β-silicon coupling constant ($a_{\beta Si} = 37.4$ G) in $(CH_3CH_2)_3SiCH_2\dot{C}H_2$ compared to the coupling of the silicon atom in the α position in the isomeric radical $(CH_3CH_2)_3Si\dot{C}HCH_3$ ($a_{\alpha Si} = 15.2$ G).[4]

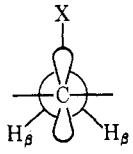

XXI

The results also indicate the presence of substantial barriers which hinder rotation about the C_α–C_β bond. It should again be possible to estimate these barriers by fitting eq 7 to the experimental temperature dependences of the β coupling constants. The question that arises is: what values of B should be chosen (A is presumably negligible) for the angular dependence of a_β (eq 8)? For radicals with methyl groups attached to the α carbon the CH_3 coupling constant can be used as a measure of B. For primary radicals such as CH_3S–$CH_2\dot{C}H_2$, however, there is no accessible internal probe.

It is possible to write empirical expressions relating the values of A and B for the series of alkyl radicals XXII which are methylated in the α position. Such a

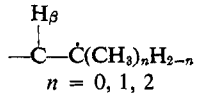

$n = 0, 1, 2$

XXII

relationship would follow from Fessenden and Schuler's suggestion[11] that each methyl group attached to an aliphatic radical center reduces the spin density on that center by a constant fraction $\Delta(CH_3)$. In the series ethyl, isopropyl, and *tert*-butyl, a value of 0.081 has been used for $\Delta(CH_3)$. Given the proportionality between the isotropic proton coupling constant and the spin density of the adjacent carbon atom we can write

$$a_{\beta n} = (A + B\cos^2\theta)(1 - \Delta(CH_3))^n = A_n + B_n\cos^2\theta \quad (9)$$

(11) R. W. Fessenden and R. H. Schuler, *J. Chem. Phys.*, **39**, 2147 (1963).

in which

$$A_n = (1 - \Delta(CH_3))^n A$$

and

$$B_n = (1 - \Delta(CH_3))^n B \quad (10)$$

where n is the number of methyl groups in XXII. For methyl groups attached to the radical center ($a_{\beta n} = a_{\beta n}{}^{CH_3}$), eq 9 implies that

$$a_{\beta n}{}^{CH_3}/a_{\beta(n-1)}{}^{CH_3} = 1 - \Delta(CH_3) \quad (11)$$

Since

$$B_n \approx 2a_{\beta n}{}^{CH_3}$$

for "freely" rotating CH_3 groups (*cf.* eq 5 with $A = 0$), it follows from eq 10 and 11 that the parameter B for a primary radical (XXII, $n = 0$) can be expressed in terms of the α-methyl coupling constants for the analogs with one ($a_{\beta 1}{}^{CH_3}$) and two ($a_{\beta 2}{}^{CH_3}$) methyl groups by eq 12.

$$B = 2(a_{\beta 1}{}^{CH_3})^2/a_{\beta 2}{}^{CH_3} \quad (12)$$

The barrier to internal rotation in a radical such as $(C_2H_5)_3SiCH_2\dot{C}H_2$ can now be determined by fitting eq 7 to the experimental temperature dependence of $a_\beta{}^{CH_2}$ (Figure 9, curve a). From the methylated analogs (Table V) we have $B = 2(24.26)^2/22.25 = 52.9$ G. The barrier height leading to a best least-squares fit is $V_0 = 1.2$ kcal/mol. We do not have complete data for the germanium and tin analogs needed to calculate the B parameters for the radicals $(C_2H_5)_3GeCH_2\dot{C}H_2$ and $(n\text{-}C_4H_9)_3SnCH_2\dot{C}H_2$. However, we have assumed B for these radicals to be unchanged, since B calculated for the silicon derivative is essentially that of the ethyl radical. The latter also suggests that Si, Ge, and Sn in the β position exert minimal inductive effects. The barrier heights obtained for $(C_2H_5)_3GeCH_2\dot{C}H_2$ and $(n\text{-}C_4H_9)_3SnCH_2\dot{C}H_2$ using this value for B are 1.6 and 2.0 kcal/mol, respectively.

The value of B for $CH_3SCH_2\dot{C}H_2$ can also be calculated from the observed CH_3 coupling constants for the methylated analogs (Table I) and eq 12. This value is again quite close to the value of B for the ethyl radical suggesting that the low values of the β-methylene coupling constants for $CH_3SCH_2\dot{C}H_2$ and related radicals cannot be ascribed to inductive effects of the sulfur atom. We would rather attribute the effect to purely geometrical considerations in which the β hydrogens are placed in positions leading to reduced hyperconjugative interactions and to rotational averaging in the presence of potential barriers.

Distortion in β-Mercaptoalkyl Radicals. The above treatment could not be extended to alkyl radicals with β-sulfur substituents since a number of anomalies were noted. Figure 9 shows that the curves for the β-methylene coupling constants for $CH_3SCH_2\dot{C}H_2$, $CH_3SCH_2\dot{C}HCH_3$, and $CH_3SCH_2\dot{C}(CH_3)_2$ [curves e, f, and g] are considerably steeper than the corresponding curves for the analogous alkyl radicals containing group IV substituents. This in itself would suggest that the β splittings are still far from their low-temperature limit. Yet the values of a_β for $CH_3SCH_2\dot{C}H_2$ (curve e) at the lowest temperatures are below the dashed line representing the approximate low-temperature limit for a primary alkyl radical. The limiting value which

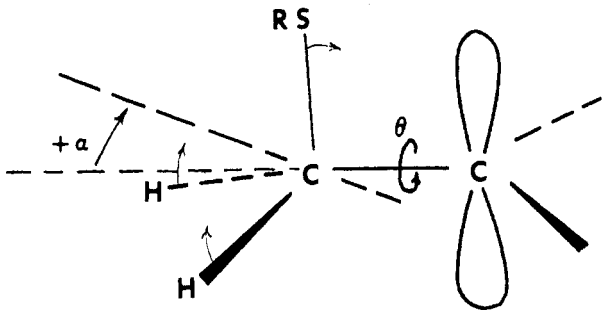

Figure 10. Distorted model for β-substituted alkyl radicals.

would be calculated from the value of B for $CH_3SCH_2CH_2\cdot$ is virtually the same. Furthermore, the situation is not improved by setting $A \neq 0$, since values of A should be positive (*vide infra*) and the limiting value ($A + {}^1/_4B$) would be even higher. Additional anomalies are evident if the data for other sulfur-alkyl radicals are considered. Thus, in Figure 9 the β splittings for $(CH_3)_3CSCH_2CH_2\cdot$ are higher (~2 G) than those for $CH_3S-CH_2CH_2\cdot$ even though their B values are essentially the same. An interesting case is the radical $CH_3SCH_2\dot{C}HCH_2-SCH_3$ which shows four equivalent β protons (at the temperatures of the experiments). The β couplings of this radical are actually higher than those of the related secondary radical $CH_3SCH_2\dot{C}HCH_3$. We again take this as evidence against any inductive effects causing the anomalously low β splittings in these radicals.

We interpret these anomalies as caused by distortions in the structures of these radicals primarily at the β carbon atom. One such distortion illustrated in Figure 10 would displace the β hydrogens away from their tetrahedral positions and toward the nodal plane. Concomitant with this distortion the sulfur atom is placed closer to the p orbital of the trigonal center. In these distorted structures the angular dependence of the hyperconjugative interactions can no longer be described by eq 1 which has heretofore formed the cornerstone of our discussion. The failure of the theory to reproduce the temperature dependence of a_β for even simple alkyl radicals (*e.g.*, isobutyl radical, Figure 6), although not as severe, may also be ascribed to departures from tetrahedral geometries and hence to the inadequacy of eq 1.

The distortion pictured above is consistent with a bonding interaction between the p orbital on the trigonal-carbon atom and the unoccupied 3d orbitals on the sulfur atom. Homoconjugation of this type has been extensively discussed in homoallylic carbonium ions[12] pictorially represented below (XXIII and XXIV).

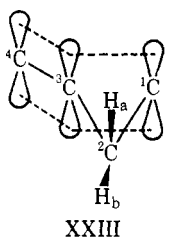

XXIII

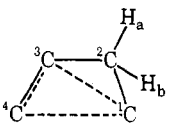

XXIV

A planar equilibrium conformation such as XXIV is also indicated for the allylcarbinyl radical ($CH_2{=}CH-CH_2CH_2\cdot$).[13] Homoconjugative interaction in this radical, however, demands an orientation of the β protons at the potential minimum corresponding to $\theta_0{}^a = \pi/6$ and $\theta_0{}^b = 5\pi/6$ (Figure 5). A similar homoconjugative interaction between the p_z orbital and the sulfur atom is qualitatively consistent with the large fluorine coupling constants observed in the $CF_3S-CH_2CH_2\cdot$ radical (Table I).

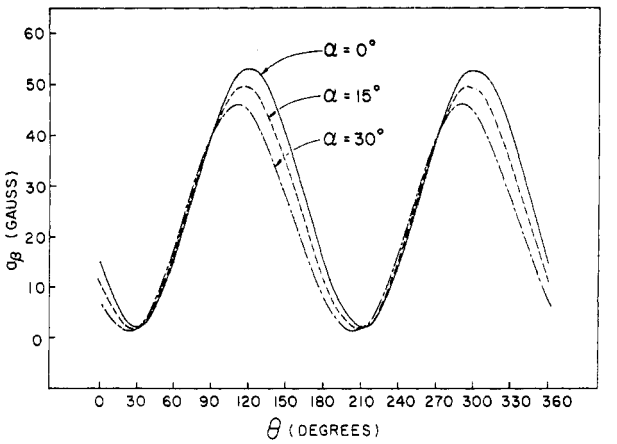

Figure 11. Angular dependences of the β coupling constants ($\theta_0 = 2\pi/3$) for the symmetric and distorted models of the ethyl radical calculated by the INDO molecular orbital method.

Distortion in Alkyl Radicals. A distorted structure of this type is the first step toward the bridged structure III previously postulated for these radicals. The larger β-methylene couplings for the *tert*-butylthiyl substituted radicals compared to the analogous methylthiyl radicals (Figure 9) can now be qualitatively understood if a smaller angle of tilt (α, Figure 10) is assumed for the analogs with the bulky *tert*-butyl group.

A quantitative treatment of hindered rotation about the $C_\alpha-C_\beta$ bond in the distorted model shown in Figure 10 requires knowledge of the angular dependence of the β-proton coupling constants (to replace eq 1). Obviously the form of this dependence cannot be obtained from the experimental data above. We revert, therefore, to theoretical predictions based on molecular orbital theory. Recently SCF-MO-LCAO calculations using the INDO empirical approximation have been quite successful in predicting isotropic hyperfine coupling constants in a large number of free radicals.[14] Unfortunately, these calculations cannot as yet be extended to radicals containing atoms of the second row of the periodic table (such as organosulfur radicals). Since the inductive effects of hetero substituents in the β position seem to be negligible and the β-methylene coupling constants are determined primarily by the geometry and rotational averaging, we have considered the ethyl radical as the simplest prototype for an examination of this question.

INDO molecular orbital calculations for the ethyl radical as a model were carried out as a function of two

(12) S. Winstein, *Quart. Rev., Chem. Soc.*, 23, 141 (1969).

(13) A measurable δ-proton interaction (0.35 G) is quite unique for acyclic alkyl radicals and supports a planar structure for this radical. This allows a measure of conjugation between the double bond and the p orbital. Two planar configurations are possible and we tentatively favor the transoid one due to the incipient antiaromatic character of the cisoid conformation [*cf.* J. K. Kochi, P. J. Krusic, and D. R. Eaton, *J. Amer. Chem. Soc.*, 91, 1877 (1969)].

(14) J. A. Pople, D. L. Beveridge, and P. A. Dobosh, *ibid.*, 90, 4201 (1968); (b) P. J. Krusic, J. P. Jesson, and J. K. Kochi, *ibid.*, 91, 4566 (1969); (c) P. Bakuzis, J. Kochi, and P. J. Krusic, *ibid.*, 92, 1434 (1970).

angles: α, the tilt of the axis of the methyl group away from the C–C internuclear direction (*cf.* Figure 10), and θ, the angle of rotation about this direction. The following assumptions were made concerning the structure of this distorted ethyl radical: a tetrahedral arrangement of the methyl protons about the axis of tilt, a planar and trigonal radical site, a length of 1.08 Å for all C–H bonds, and a C–C bond length of 1.58 Å. The calculated coupling constants for the β proton with phase $\theta_0 = 2\pi/3$ in the equilibrium conformation (Figure 5) for the symmetric ($\alpha = 0°$) and for the two distorted ($\alpha = +15$ and $+30°$) ethyl radicals are shown in Figure 11. A number of features emerge. The curve for the symmetric ethyl radical can be fitted quite closely by eq 1 with $A = 2.2$ G and $B = 50.9$ G in agreement with our previous knowledge of these parameters. This corresponds to an isotropic average ($A + 0.5\ B$) of 27.6 G which compares quite well with the experimental value $a_\beta = 26.8$ G for the ethyl radical. The curves for the distorted radicals, on the other hand, cannot be represented by a simple $\cos^2$ law. More importantly, the expected diminution of a_β is obtained at the equilibrium conformation ($\theta = 0$) for $\alpha > 0$.

We can now consider the effects of anisotropic rotational averaging on the β splittings for a distorted model whose angular dependence is given by the curves of Figure 11. The classical anisotropic averaging of eq 7 can still be carried out by a computer with the angular dependence of a_β expressed in numerical rather than analytical form. The temperature dependences of a_β calculated in this manner for a barrier height of 1500 cal/mol are shown in Figure 12 together with the experimental points for the $CH_3SCH_2CH_2\cdot$ radical. Also shown is the low-temperature limit inferred from $a_\beta^{CH_3}$ for the ethyl radical. It is seen that a distorted model can predict β coupling constants below this limit and even predict a slope of the temperature dependence which is similar to the experimental one. Unfortunately, the two parameters of the model, α and V_0, cannot be determined simultaneously from the experimental data. The values of α and V_0, however, should be in the range 15–30° and 1–2 kcal/mol, respectively.

We conclude with a few remarks about the simple acyclic hydrocarbon radicals considered earlier. We saw in Figure 6 that both the quantum mechanical treatment and our classical treatment failed to reproduce the experimentally observed slopes of the temperature dependences of a_β. For example, the experimental curve for a_β in the isobutyl radical is considerably steeper than the curve calculated on the basis of the $\cos^2$ angular relationship for a_β. Such a slope, however, is predicted if the axis of the $(CH_3)_2CH$– group is tilted by a positive angle α (compare Figure 10) in that conformation in which the single β proton is eclipsed by the p orbital. Such a distortion would lengthen the distance between the two methyl groups and the α protons but, at the same time, bring the β proton closer to the p orbital. Although precise values for α and V_0 cannot be given it is clear that a bent distorted model does give a better fit to the experimental curves.

These arguments are also supported by consideration of the *tert*-amyl radical whose equilibrium conformation is given by XX. The experimental curve for $a_\beta(T)$ given in Figure 6 for the *tert*-amyl radical is *less steep* than the calculated one. We find that a small tilt in the negative direction ($\alpha < 0$, *cf.* Figure 10) produces a correct change in the slope of the calculated temperature dependence. This operation takes the γ-methyl group farther from the p orbital and hence further from the α-methyl groups.

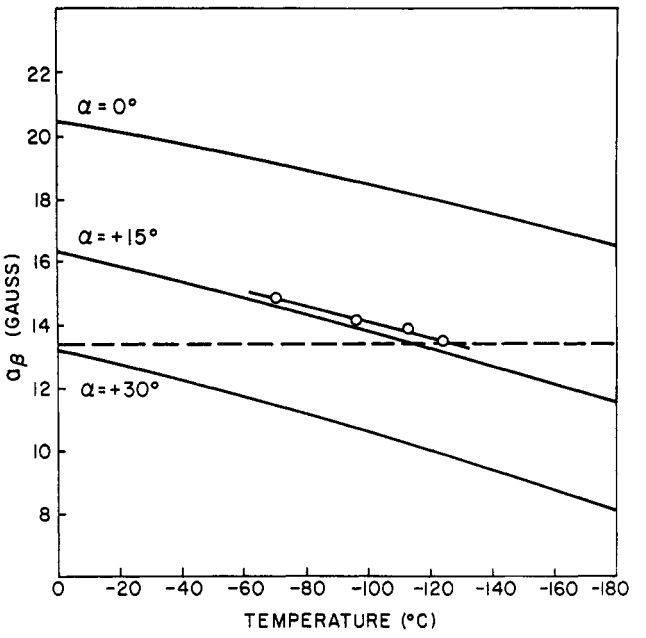

Figure 12. Calculated temperature dependences of the β coupling constant ($\theta_0 = 2\pi/3$) for the symmetric and distorted models of the ethyl radical assuming a barrier of 1500 cal/mol. Open circles are the experimental values of a_β for $CH_3SCH_2CH_2\cdot$. Dashed line represents the low-temperature limit estimated from the experimental $a_\beta^{CH_3}$ in the ethyl radical.

Conformations of Simple Alkyl Radicals by Line-Broadening Effects. Conformations of alkyl radicals can also be deduced by the observations of selective line-broadening effects in the esr spectrum.[15] For example, the esr spectrum of *n*-propyl radicals at $-140°$ is shown in Figure 7. The central lines ($M_I = 0$) of the triplet splitting corresponding to the α protons are broadened and appear with reduced peak-to-peak amplitudes. The triplets corresponding to a_β have their relative intensities. The β protons are thus equivalent whereas the α protons are exchanging between two different environments at a rate comparable to the difference in the splittings for the two sites. These conditions are met by exchange between the two equilibrium conformations XXV and XXVI in which the γ-methyl group is eclipsed by an α proton. The same conclusion was arrived at on the basis of the magnitudes of the β coupling constants (*vide supra*).

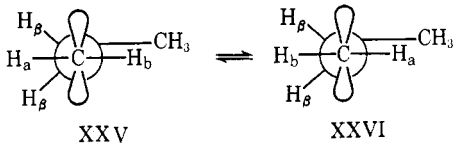

XXV XXVI

The *n*-butyl radical (Figure 13) exhibits the opposite behavior. The central lines of the triplets

(15) (a) C. S. Johnson, *Advan. Magn. Resonance*, **1**, 33 (1965); (b) A. Hudson and G. R. Luckhurst, *Chem. Rev.*, **69**, 191 (1969); (c) D. H. Geske, *Progr. Phys. Org. Chem.*, **4**, 125 (1967); P. D. Sullivan and J. R. Bolton, *Advan. Magn. Resonance*, **4**, 39 (1970).

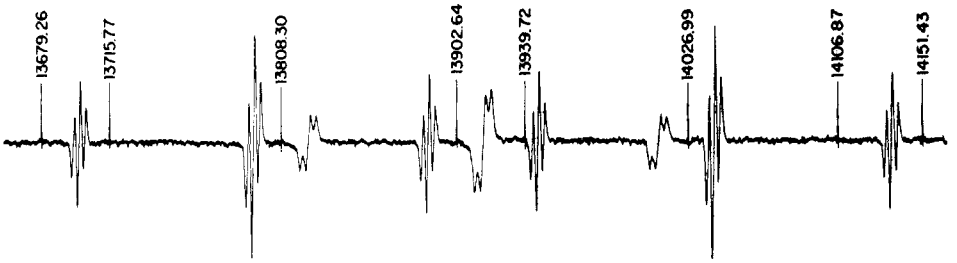

Figure 13. Esr spectrum of *n*-butyl radical from the photolysis of a solution of *n*-valeryl peroxide in cyclopropane at −105°.

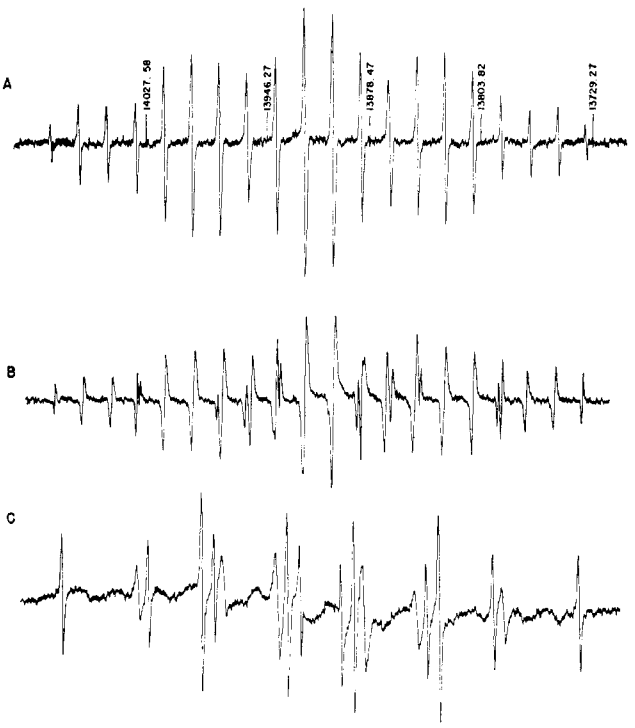

Figure 14. Esr spectrum of $CF_3SCH_2CH_2\cdot$ from the addition of trifluoromethylthiyl radical to ethylene at (A) −102°, (B) −127°, and (C) −162°. Changes in the spectrum are associated with (a) temperature-dependent β-methylene coupling constant and (b) alternating line-width effect due to hindered rotation of the CF_3 group.

corresponding to the β-proton splitting are broader than the corresponding lines for the α-proton coupling. An internal rate process in this radical exchanges the β protons between different environments. Hindered rotation about the C_β–C_γ bond is consistent with this exchange. Examination of molecular models indeed shows that a rotation of the kind illustrated below is sterically hindered. The configuration pictured above

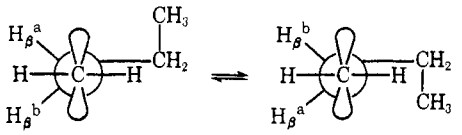

is also consistent with quite similar β coupling constants for *n*-propyl and *n*-butyl radicals (~30 G at −100°). Noteworthy is the larger γ-proton splitting in *n*-butyl (0.7 G) compared to that in *n*-propyl (0.3 G) radical.

The absence of line-width variations in isobutyl and *tert*-amyl radicals as well as in the various β-substituted alkyl radicals with S, Si, Ge, and Sn substituents is consistent with the symmetric equilibrium conformation discussed earlier. This is no longer true when the β heteroatom is oxygen or nitrogen. Thus, Livingston and Zeldes[5] reported a β coupling constant of 31.7 G at −71° in $HOCH_2CH_2\cdot$ (*cf.* $a_\beta \sim 14$ G in $CH_3SCH_2CH_2\cdot$). We have obtained the same spectrum by photolyzing static solutions of hydrogen peroxide in ethanol. The β splitting for this radical *increases* as the temperature is lowered and a pronounced broadening of the $M_I = 0$ lines associated with the α protons is observed. An equilibrium conformation analogous to that of *n*-propyl radical is indicated with the oxygen atom eclipsing the α hydrogen. The same conformation (with the oxygen in the nodal plane of the π system) must also exist for β-trifluoromethoxy and β-methoxyethyl radicals (Table VI). We infer from the magnitude of the β-coupling constant[8] reported for $H_2NCH_2CH_2\cdot$ that this radical also possesses an analogous conformation.

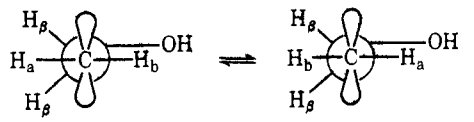

The β-Trifluoromethylthiylalkyl Radicals. The esr spectrum at several temperatures of the β-trifluoromethylthiylethyl radical XXVII derived by addition of the trifluoromethylthiyl radical to ethylene is shown in Figure 14. The temperature dependence of the β coupling constant (shown clearly in Figure 14A and B) is entirely analogous to that discussed earlier for other β-thiylalkyl radicals. In addition, there are two further features in the spectrum of this radical which are noteworthy: (a) a dramatic broadening of the lines corresponding to $M_I = \pm 0.5$ of the quartet splitting due to the three equivalent fluorine atoms, indicative of restricted rotation of the trifluoromethyl group and (b) the $M_I = 0$ lines of the triplets associated with the β protons are also broadened at −162° (Figure 14C) indicative of a modulation of the β coupling constant caused by hindered internal rotation of the trifluoromethyl group about the C_β–S bond. The conformation shown in XXVII is also consistent

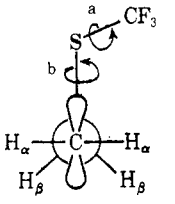

XXVII

with the much larger fluorine coupling constant in this radical compared to the oxygen analog mentioned above

in which the oxygen atom lies in the nodal plane. Furthermore, the absence of the line-width effect in the fluorine quartet indicates that rotation about the CF_3–O bond is virtually unhindered even at temperatures as low as −140°.

Line broadening is absent in the spectrum of $CH_3SSCH_2\cdot$ (a_α = 17.34 G at −130°) obtained from dimethyl disulfide. We conclude that this radical exists in a symmetric conformation analogous to the β-mercaptoalkyl radical discussed above. Similar conformational effects were discussed earlier with $(CH_3)_3COCH_2\cdot$ and $(CH_3)_3SiOCH_2$.[4] However, in the α-substituted methylthiylmethyl radical XXVIII, an asym-

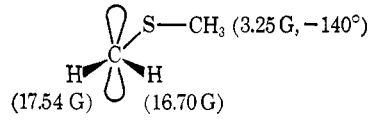

XXVIII

metric conformation is implied by the broadening of the central lines (M_I = 0) of the α triplet. The broadening is followed by a resolution into the slow exchange limit shown in Figure 15. This radical, therefore, exists in a planar conformation promoted by partial double bonding between the trigonal-carbon atom and the sulfur atom. Stabilization associated with such electron delocalization is represented by the valence-bond formulations XXIX and is manifested in the

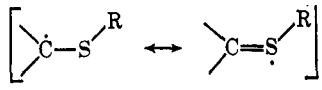

XXIX

well-known chemical reactivity of the α position of thioethers.[16] A similar situation pertains to the oxygen analogs derived from alcohols and ethers.[17]

The Mercaptoallyl Radical VIII. An interesting combination of a line-width effect and a temperature-dependent coupling constant occurs in the esr spectrum of the adduct VIII of methylthiyl radical to 1,3-butadiene discussed above. A cursory examination of the spectrum obtained at −120° leads to the conclusion that only *one* of the methylene hydrogens is involved in the splitting. At higher temperatures (−10°), however, an additional line appears at the median position of this "doublet" throughout the spectrum. At intermediate temperatures the extra line is severely broadened and reduced in amplitude. These "doublets" are clearly the sharp lines of an exchange-broadened triplet.

This behavior is consistent with an exchange between two equivalent equilibrium conformations represented by XXX and XXXI. The magnitude of the observed

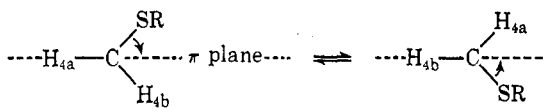

XXX XXXI

temperature-dependent triplet splitting ($a_{H_4} \simeq 9$ G) represents an averaged value $[0.5(\langle a_{H_{4a}}\rangle + \langle a_{H_{4b}}\rangle)]$ for the two nonequivalent protons. The larger values

(16) *Cf.* also A. Ohno and Y. Ohnishi, *Tetrahedron Lett.*, 4405 (1969).
(17) A. Hudson, *J. Chem. Soc. A*, 2513 (1969); P. J. Krusic, P. Meakin, and J. P. Jesson, Abstracts, 159th National Meeting of the American Chemical Society, Houston, Tex., Feb 1970, No. PHYS 033.

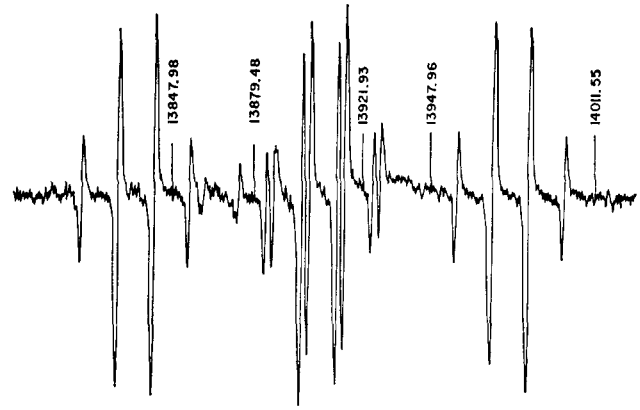

Figure 15. Esr spectrum of $CH_3SCH_2\cdot$ obtained by reaction of *tert*-butoxy radicals with dimethyl sulfide at −140° showing inequivalence of the α protons.

for equivalent H_4 protons in the 1-pentenyl (a_{H_4} = 14 G) and 4-*tert*-butoxy-1-butenyl V (a_{H_4} = 16 G) radicals leads us to conclude that these radicals prefer the conformations XXXII and XXXIII. The unique position occupied by the sulfur atom in XXX and XXXI is, of course, related to the equilibrium conformations of the β-mercaptoalkyl radicals discussed earlier.

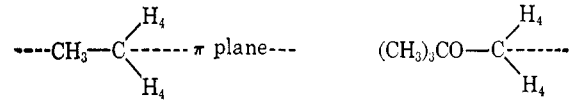

XXXII XXXIII

Summary and Conclusions

The esr spectra of a series of alkyl radicals hetero-substituted in the β position with sulfur, silicon, germanium, and tin show unusual values of the β-proton coupling constants compared to their alkyl and β-oxy analogs. These coupling constants also exhibit unusually large temperature dependences. In alkyl radicals the magnitudes of the coupling constants of the β proton are dependent on its orientation relative to the p orbital and are, therefore, directly related to the rotational conformation of the species. The temperature dependence of the β coupling constant $[a_\beta(T)]$ is associated with the barrier to internal rotation around the C_α–C_β bond and can be treated theoretically. We have extended the theory of motional averaging of the β coupling constant in the presence of a twofold potential. The values of $a_\beta(T)$ for these radicals obtained in this manner can be fitted to the experimental curves to obtain the heights of the barriers hindering rotation. In the conformation at the potential minimum the β heteroatom eclipses the p orbital on the radical center. The unusually low values of the β coupling constants for the β-alkylmercaptoethyl radicals are predicted by a model in which the β-sulfur atom is displaced from its tetrahedral position toward the p orbital. These radicals are not truly bridged structures but rather exist in preferred conformational orientations which may be sufficient to control stereochemistry. These conclusions regarding the conformational effects exerted by β-sulfur substituents are also consistent with line broadening observed in the esr spectra of sulfur-substituted allyl radicals and trifluoromethylthiyl-substituted ethyl radicals.

Acknowledgment. We wish to thank Mr. Kenneth Eaby for technical assistance and Dr. Walter Mahler for helpful discussions and a sample of bistrifluoromethyl disulfide. We also thank Dr. Paul Meakin for his help and interest and Mr. N. McGowan for his contribution to the construction of the field marker.

An Infrared Spectroscopic Study of the Photolytic Decomposition of Methyl Azidoformate[1]

R. E. Wilde,*[2a] T. K. K. Srinivasan,[2a] and Walter Lwowski[2b]

Contribution from the Departments of Chemistry, Texas Tech University, Lubbock, Texas 79409, and New Mexico State University, Las Cruces, New Mexico 88001.
Received July 29, 1970

Abstract: Methyl azidoformate has been photolyzed in rare-gas matrices near 4°K and in the solid state at 77°K. Methoxy isocyanate, formaldehyde, and isocyanic acid are proposed as possible photolysis products which are consistent with the infrared spectra. Mechanisms based on band-intensity changes upon prolonged photolysis are also proposed.

Several investigations of the photolysis of the alkyl azidoformates[3-8] have led to a much better understanding of the mechanisms involved. It has become clear that singlet nitrene plays an important role in the photolytic decomposition of the alkyl azidoformates. It has also been discovered recently that these so-called "rigid" azides undergo rearrangement in hydroxylic solvents[9] as well as hydrocarbon solvents.[10]

In an effort to better understand the intermediates involved in the photolysis of the alkyl azidoformates, methyl azidoformate and methyl azidoformate-d_3 were photolyzed in rare-gas matrices near 4°K. The decompositions were studied by means of infrared spectroscopy. The methyl species was chosen for study because of its simpler spectrum.

Experimental Section

Methyl azidoformate-d_3 was obtained by introducing 0.056 mol of methanol-d_3 into a solution of 30 g of phosgene in 50 ml of anhydrous ether at 0°, refluxing the mixture, then distilling the solvent and excess phosgene over a 12-in. helix-packed column. The pot residue was dissolved in ether and stirred with an aqueous solution of a small excess of sodium azide at 0° for 20 hr. Distillation of the ether and microdistillation of the residue at 40° (55 mm) gave 1.8 g (42% yield) of pure methyl azidoformate-d_3. We are greatly indebted to Dr. S. M. A. Hai for carrying out this preparation.

The methyl azidoformate was kept below 0° and protected from light until needed. All manipulations of the methyl azidoformate were carried out in high vacuum. One sample remained in the high-vacuum system at room temperature and unprotected from light for 6 months; no decomposition could be detected spectroscopically.

The methyl azidoformate was mixed with neon and argon at concentrations of 0.25–0.1 mol % azidoformate. The gases were allowed to mix for at least 24 hr before deposition.

Isocyanic acid was prepared according to the method employed by Herzberg and Reid.[11] Formaldehyde vapor was produced by heating paraformaldehyde (polyoxymethylene) until the required pressure of the vapor was obtained.

The cryostat employed was an Andonian Modular Design[12] with rotatable tail section designed to fit into the optical system of the Beckman IR-9 spectrophotometer. Temperature control was accomplished using the Teflon-plug technique[13] in conjunction with a 20-ohm resistance heater located immediately above the deposition-window frame. The temperature was measured with a Cryo resistor[14] mounted on the deposition-window frame. The temperature of the sample when in the infrared beam was estimated to be 6°K.

The photolysis was carried out through a fused-quartz window with a General Electric H4AB low-pressure mercury lamp from which the Pyrex envelope had been removed. The beam was focused with a spherical mirror so that the focal point was just behind the deposition window, thereby allowing the entire sample area to be exposed to the radiation.

All spectra were obtained with a Beckman IR-9 spectrophotometer. Under the experimental conditions, the probable error in the wave number is estimated to be ± 1 cm^{-1} throughout the spectral range (400–4000 cm^{-1}).

Results

Comparison of the gas-phase and matrix-isolation infrared spectra of methyl azidoformate shows that the same number of bands with the same relative intensities are present in both the gas-phase and matrix-isolation spectra. The spectra of methyl azidoformate and its photolysis products are the same in both neon and argon matrices, except for small solvent shifts. For this reason, only the vibrational wave numbers of the neon-isolated samples are reported. The wave numbers of all new bands appearing in the neon matrix are listed

(1) This research was partially supported by a grant from the Robert A. Welch Foundation.
(2) (a) Texas Tech University; (b) New Mexico State University.
(3) W. Lwowski and T. Mattingly, Jr., *Tetrahedron Lett.*, 277 (1962).
(4) R. S. Berry, D. Cornell, and W. Lwowski, *J. Amer. Chem. Soc.*, **85**, 1199 (1963).
(5) W. Lwowski, T. J. Maricich, and T. W. Mattingly, Jr., *ibid.*, **85**, 1200 (1963).
(6) W. Lwowski, T. W. Mattingly, Jr., and T. J. Maricich, *Tetrahedron Lett.*, 1591 (1964); J. Hancock, *ibid.*, 1585 (1964).
(7) W. Lwowski and T. W. Mattingly, Jr., *J. Amer. Chem. Soc.*, **87**, 1947 (1965).
(8) D. W. Cornell, R. S. Berry, and W. Lwowski, *ibid.*, **87**, 3626 (1965).
(9) W. Lwowski, R. DeMauriac, T. W. Mattingly, Jr., and E. Scheiffele, *Tetrahedron Lett.*, 3285 (1964).
(10) R. Puttner, W. Kaiser, and K. Hafner, *ibid.*, 4315 (1968).
(11) G. Herzberg and C. Reid, *Discuss. Faraday Soc.*, **9**, 92 (1950).
(12) Andonian Associates, Waltham, Mass.
(13) R. Savoie and A. Anderson, *J. Chem. Phys.*, **44**, 548 (1966).
(14) Cryo Cal, Inc., Riviera Beach, Fla.